

RNAi-Mediated β -Catenin Inhibition Promotes T Cell Infiltration and Antitumor Activity in Combination with Immune Checkpoint Blockade

Shanthi Ganesh,¹ Xue Shui,¹ Kevin P. Craig,¹ Jihye Park,¹ Weimin Wang,¹ Bob D. Brown,¹ and Marc T. Abrams¹

¹Dicerna Pharmaceuticals, Inc., Cambridge, MA 02140, USA

Wnt/ β -catenin signaling mediates cancer immune evasion and resistance to immune checkpoint therapy, in part by blocking cytokines that trigger immune cell recruitment. Inhibition of β -catenin may be an effective strategy for increasing the low response rate to these effective medicines in numerous cancer populations. DCR-BCAT is a nanoparticle drug product containing a chemically optimized RNAi trigger targeting *CTNNB1*, the gene that encodes β -catenin. In syngeneic mouse tumor models, β -catenin inhibition with DCR-BCAT significantly increased T cell infiltration and potentiated the sensitivity of the tumors to checkpoint inhibition. The combination of DCR-BCAT and immunotherapy yielded significantly greater tumor growth inhibition (TGI) compared to monotherapy in B16F10 melanoma, 4T1 mammary carcinoma, Neuro2A neuroblastoma, and Renca renal adenocarcinoma. Response to the RNAi-containing combination therapy was not dependent on Wnt activation status of the tumor. Importantly, this drug combination was associated with elevated levels of biomarkers of T cell-mediated cytotoxicity. Finally, when CTLA-4 and PD-1 antibodies were combined with DCR-BCAT in MMTV-Wnt1 transgenic mice, a genetic model of spontaneous Wnt-driven tumors, complete regressions were achieved in the majority of treated subjects. These data support RNAi-mediated β -catenin inhibition as an effective strategy to increase response rates to cancer immunotherapy.

INTRODUCTION

Tumors evade the immune system, in part, by activating molecular checkpoints that dampen antitumor host defense responses.¹ Pharmacological blockade of these inhibitory checkpoints promotes tumor cell lysis by activation of cytotoxic T cells in response to the presentation of tumor antigens.^{2,3} The recent development and commercialization of cancer immunotherapeutics, including PD-1-, PD-L1-, and CTLA-4-targeting antibodies, have led to dramatically increased response rates in melanoma and several other tumor types.⁴ However, most tumors remain insensitive to checkpoint blockade immunotherapy. A primary determinant of response to checkpoint blockade is the presence of an inflamed microenvironment containing T cells, elevated levels of interferon (IFN) γ , and elevated levels of PD-L1.⁵ Non-inflamed tumors, also referred to as immunologically cold, respond poorly to immunotherapy, in part

due to their lack of sufficient T cell content in the microenvironment.⁶ Recent efforts to increase the low response rates to cancer immunotherapeutics have included combining multiple checkpoint inhibitors, which increased efficacy but also increased the occurrence of immune-related adverse effects.⁷ Other efforts to sensitize cancers to checkpoint blockade are in early clinical evaluation, including combining with standard-of-care chemotherapy,⁸ radiotherapy,⁹ or targeted small molecule inhibitors of epigenetic modifiers¹⁰ and signaling kinases.¹¹

The Wnt/ β -catenin pathway, a signaling network with broad roles in development and homeostasis, is strongly tumorigenic when dysregulated.¹² Aberrant accumulation of β -catenin in the cell nucleus, caused by mutations in the protein itself or in direct binding partners, promotes a transcriptional program that serves as a key driver of transformation, tumor maintenance, and metastasis. More recently, β -catenin has been directly implicated in tumor immunology, particularly in melanoma. These observations culminated in the demonstration by Spranger et al.¹³ that Wnt/ β -catenin pathway signatures are inversely correlated to T cell signatures in biopsies from metastatic melanoma patients. Furthermore, genetic activation of β -catenin excluded T cells from mouse melanoma tumors and rendered them insensitive to PD-1 and CTLA-4 antibodies. Importantly, mutations in Wnt-related genes correlated strongly to a low T cell signature in a large panel of human colorectal tumors.¹⁴ One mechanism by which β -catenin promotes immune cell evasion is proposed to involve the upregulation of transcriptional repressor ATF3, which in turn prevents the tumor cell from secreting CCL4, a chemokine attractant that allows antigen-presenting cells to infiltrate the tumor.¹³ This is likely to be one of several strategies by which oncogenic pathway activation or suppression can regulate consequential interactions with immune cells in the tumor microenvironment (TME). In addition to β -catenin, recent observations suggest that RAS/MAPK,¹⁵ PTEN,¹⁶ and MYC¹⁷ signaling may also have immune-modulating functionality.

Received 23 April 2018; accepted 6 September 2018;
<https://doi.org/10.1016/j.ymthe.2018.09.005>

Correspondence: Shanthi Ganesh, Dicerna Pharmaceuticals, Inc., 87 Cambridgepark Drive, Cambridge, MA 02140, USA.

E-mail: sganesh@dicerna.com



While several indirect Wnt pathway inhibitors are in various stages of clinical development,¹² efforts to block β -catenin directly using conventional pharmaceutical modalities have not been successful. RNAi is an emerging technology, enabling the inhibition of traditionally undrug-treatable targets at the mRNA level.¹⁸ We have previously reported the development of a potent RNAi trigger targeting *CTNNB1*, the gene that encodes β -catenin.¹⁹ The drug product containing this oligonucleotide, termed DCR-BCAT, is an intravenously delivered lipid nanoparticle (LNP) formulation that selectively silences *CTNNB1* in tumors and causes rapid tumor growth inhibition in diverse Wnt-dependent preclinical models. In the preclinical setting, DCR-BCAT is efficacious against primary and metastatic tumors, both as a monotherapy and in combination with conventional targeted therapeutics at well-tolerated doses.^{19,20}

In this report, we demonstrate that DCR-BCAT treatment causes robust increases in tumor-associated T cell content, antigen-presenting cells (APCs), immune checkpoint expression, and chemokine expression in murine tumors. In syngeneic models of melanoma, renal, neuroblastoma, and mammary carcinomas, combining immunotherapy with DCR-BCAT sensitized non-inflamed tumors and demonstrated synergistic efficacy. In spontaneous Wnt1-driven mammary tumors, DCR-BCAT plus PD-1/CTLA-4 therapy yielded complete regressions in the majority of treated animals. These data suggest *CTNNB1* RNAi therapy as an effective approach to improve response rates to immunotherapy for cancers of diverse genetic origin.

RESULTS

RNAi-Mediated β -Catenin Inhibition Increases T Cell Infiltration in Immunotherapy-Refractory Syngeneic Mouse Tumors

RNAi therapy is an approach to post-transcriptionally silence mRNAs with high potency and specificity. Dicer-substrate small interfering RNAs (siRNAs) (DsiRNAs) targeting *CTNNB1*, formulated in a tumor-selective lipid nanoparticle, cause robust suppression of Wnt/ β -catenin effectors and proliferation of Wnt-dependent tumors in preclinical models at well-tolerated dose levels.¹⁹ This experimental drug product, termed DCR-BCAT, also displays synergistic efficacy in combination with other oligonucleotides and targeted MAPK pathway inhibitors.²⁰ The DCR-BCAT DsiRNA contains stabilizing and immune-evading ribose modifications (2'-O-Me and 2'-F nucleosides), and the RNAi target site is 100% conserved between the human *CTNNB1* gene and the murine *Ctnnb1* gene, enabling experimental use in tumors derived from both species.¹⁹

In the context of recent hypotheses around the role of β -catenin in tumor immunology,¹³ we sought to investigate whether specific pharmacological inhibition of *Ctnnb1* mRNA impacts immune cell subpopulations and relevant signaling intermediates in a model of murine melanoma. B16F10 tumors, known to be refractory to immune checkpoint therapy,²¹ were allografted subcutaneously into immunocompetent C57BL/6 mice. After the tumors reached a volume of 250 mm³, DCR-BCAT or DCR-Placebo (a scrambled DsiRNA with matched chemistry and formulation), along with a separate

vehicle control, were administered intravenously via tail vein, according to the dosing regimen shown in Figure 1A (n = 5–6/cohort). Tumors were excised for pharmacodynamic endpoint analysis after treatment. qPCR measurements using total RNA isolated from the tumor show that DCR-BCAT caused a partial reduction in *Ctnnb1* mRNA and a concomitant increase in the *Ccl4* mRNA (Figure 1B). As β -catenin has been previously shown to cause immune evasion, in part, by transcriptional repression of *Ccl4*, the alleviation of *Ccl4* repression is associated with robust increases in the dendritic cell mRNA marker *Itgae*, which encodes CD103, and the cytotoxic T cell mRNA marker *Cd8a* (Figure 1B). These RNAi effects generally confirm previous observations reported using a model where activated *Ctnnb1* was genetically introduced into murine melanoma.¹³

We then performed flow cytometry to measure surface markers on single-cell suspensions prepared from the extracted B16F10 tumors (Figure 1C). While the irrelevant DsiRNA placebo had no significant effect on the tumor immune compartment, DCR-BCAT treatment resulted in highly significant increases in total T cells (CD3), cytotoxic T cells (CD8), antigen-presenting dendritic cells (CD103), and the PD-1 T cell checkpoint. Additional flow cytometry analyses showed a treatment-associated increase in three different T cell receptor (TCR) cofactors known to be checkpoints within CD8+ T cells: PD-1, TIM-3, and LAG-3 (Figure S1A). In contrast to the robust increase in tumor T cell content, there were no observed treatment-related effects on tumor-associated natural killer (NK) cells, another important subpopulation known to modulate response to immunotherapy (Figure S1B).²² Similarly, changes in immunosuppressive myeloid-derived suppressor cells (MDSCs) and regulatory T cells (T_{regs}) after treatment were minimal and variable (Figure S1B). These data suggest that recruitment of cytotoxic T cells is a dominant mechanism of immunomodulation by β -catenin RNAi therapy.

Finally, immunohistochemistry (IHC) for β -catenin and CD8 proteins, performed on formalin-fixed, paraffin-embedded (FFPE) B16F10 tumor tissue, provided further confirmation of the DCR-BCAT treatment effects (Figure 1D). For both the IHC and flow cytometry datasets, the tumor samples were derived from separate, independent in-life experiments. Loss of β -catenin protein after RNAi therapy (approximately 60% decrease in relative intensity) was homogeneous throughout the tumor section, and it was observed in both the cell membrane and the cytosol of B16F10 tumors. In the native state, the tumors are negative for CD8, consistent with their immunologically cold status. After two rounds of DCR-BCAT treatment, CD8 staining was observed throughout the tumor (Figure 1D). Collectively, the qPCR, flow cytometry, and IHC data demonstrate the potential of RNAi silencing of *Ctnnb1* to increase the population of tumor-associated APCs and lymphocytes, both of which are known to have positive predictive value for response to immunotherapy.

RNAi-Mediated β -Catenin Inhibition Potentiates the Activity of Immune Checkpoint Inhibitors in Syngeneic Tumors

While immune checkpoint blockade has demonstrated a clear benefit for patients experiencing a subset of melanoma, lung, and other

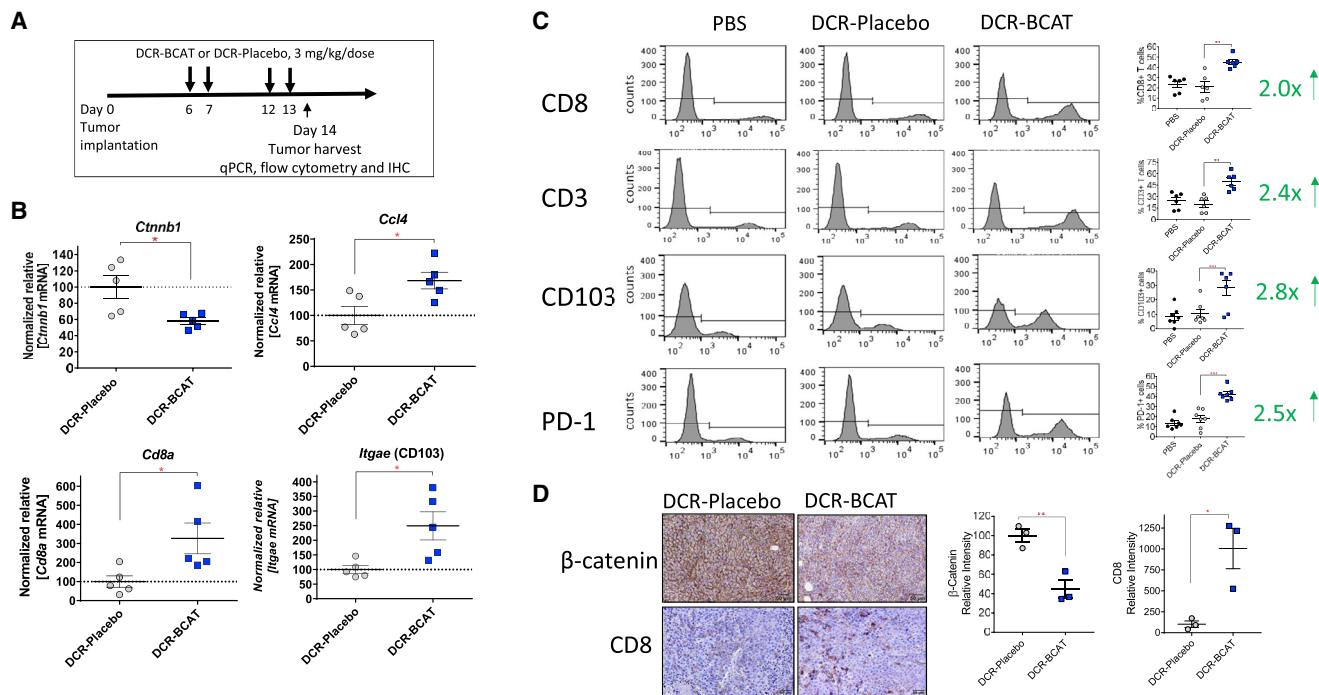


Figure 1. β-Catenin Inhibition Increases Immune Cell Infiltration in B16F10 Tumors

(A) C57BL/6 mice were subcutaneously allografted with 1×10^6 B16F10 cells and dosed intravenously with DCR-BCAT or DCR-Placebo using the regimen outlined. (B) Tumors were extracted 24 hr after the final of 4 doses. Total RNA was extracted and subjected to qPCR analysis for relative expression of specific mRNAs as indicated. (C) Flow cytometry quantitation of 4 analytes: CD8 for cytotoxic T cells, CD3 for total T cells, and CD103 for dendritic cells and the PD-1 checkpoint. Representative histograms are displayed, as well as dot plots showing the measurements for all animals on study. Green text indicates the mean fold elevation of each marker for the DCR-BCAT cohort versus DCR-Placebo cohort. (D) Representative immunohistochemical staining for mouse β-catenin (top scale bars: 50 μm) and CD8 (bottom scale bars: 50 μm) in FFPE sections prepared after the dosing regimen outlined in (A). Relative intensity quantitation for all animals is shown on the right panel. $n = 5$ for qPCR experiments, $n = 6$ for flow cytometry experiments, $n = 3$ for immunohistochemistry; error bars represent the SEM; * $p < 0.05$, ** $p < 0.01$, *** $p < 0.001$ by unpaired t test and one-way ANOVA.

tumors, most tumors are non-responsive.^{23,24} Likewise, many experimental murine tumor models are also insensitive or only partially sensitive to immunotherapy, and the majority of preclinical study has focused on a small subset of models to demonstrate the efficacy of these agents. Given the ability of RNAi-mediated β-catenin inhibition to increase tumor-associated cytotoxic T cells, we sought to determine if DCR-BCAT could sensitize refractory tumors to a standard immunotherapy regimen containing anti-PD-1 and CTLA-4 antibodies.

In Figure 2A, immunocompetent mice harboring subcutaneous B16F10 tumors were treated systemically with DCR-BCAT or the formulated placebo DsiRNA (DCR-Placebo), followed by the immune checkpoint inhibitors, for two cycles over 2 weeks. The rationale for the dosing regimen was that RNAi therapy would have to be administered first in each cycle, to enable T cell recruitment to the tumor, before initiating checkpoint blockade. The selection of anti-PD-1/CTLA-4 and the immunotherapy dose regimen employed in these studies was made based on previous work from Spranger et al.,¹³ where it was evaluated in a preclinical melanoma model that had been engineered to express an activated allele of *Ctnnb1*.

Immunotherapy alone (in combination with a placebo DsiRNA) yielded only 50% tumor growth inhibition, as expected based on previously reported observations for this model.²⁵ DCR-BCAT alone was ineffective, as expected since β-catenin inhibition as a single agent was shown to only be efficacious in tumors with dysregulated Wnt signaling and detectable nuclear β-catenin, a category that includes 90% of colorectal tumors but few melanomas.^{19,26,27} However, combining the two agents resulted in synergistic efficacy and near-complete tumor growth inhibition (Figure 2A). To determine if the benefits of combination therapy are unique to melanoma or unique to the properties of B16F10 tumors, we performed a similar study in a second syngeneic allograft model, Neuro2A neuroblastoma, which has been recently shown to be unresponsive to PD-1 therapy.²⁸ While no activity was observed with either DCR-BCAT or immunotherapy alone, 74% tumor growth inhibition (TGI) was achieved in combination (Figure 2B).

To determine if the mechanism of action for combination treatment involves cytotoxic T cell-mediated tumor cell death, we performed immunohistochemistry for granzyme B and perforin (Figures 2C and 2D). Following antigen recognition by CD8+ T cells,

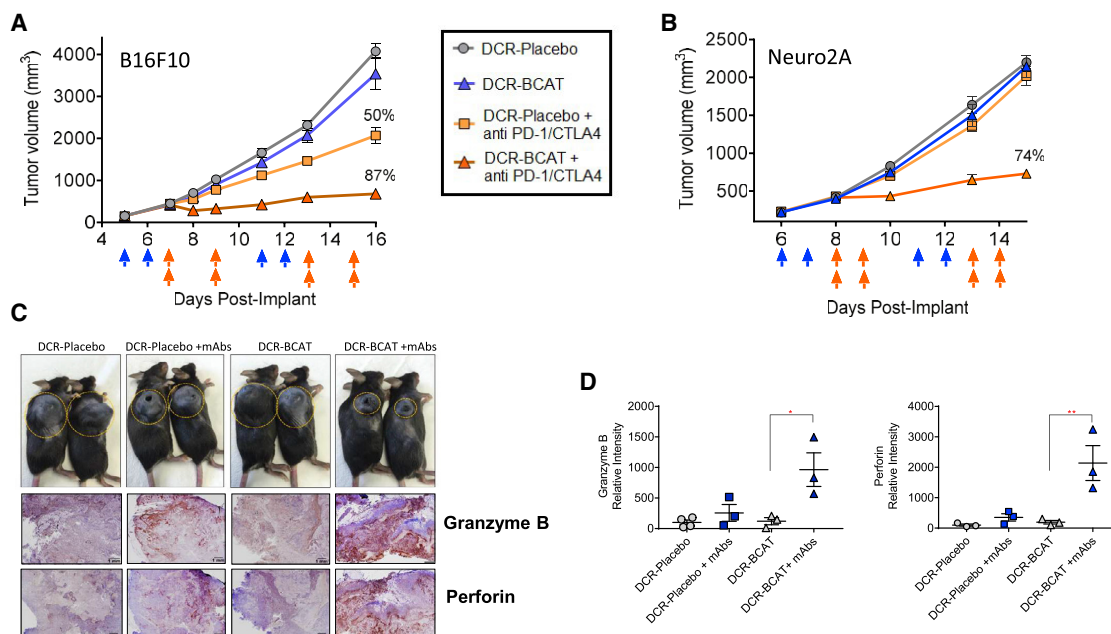


Figure 2. DCR-BCAT Sensitizes Syngeneic Tumors to Immune Checkpoint Blockade

B16F10 (A) or Neuro2A (B) tumor-bearing mice ($n = 5/\text{cohort}$) were generated and enrolled as described in Figure 1. The range of tumor volumes at the time of dosing was 100–200 mm³ for B16F10 and 200–300 mm³ for Neuro2A. Animals were dosed on the days indicated by the arrows (blue arrows, DCR-BCAT or DCR-Placebo, 3 mg/kg/dose; orange arrows, anti-PD-1/CTLA-4, 5 mg/kg/dose of each antibody in the combination cohorts only as indicated in the figure). DCR-BCAT and DCR-Placebo were given intravenously (tail vein) and the antibodies were administered intraperitoneally. Tumor volumes were measured twice weekly over the study period. The mean TGI values are displayed on the plots for the cohorts that responded to therapy. (C) Whole-animal photograph of B16F10 animals on study at the terminal time point, day 16 ($n = 2/\text{cohort}$), with the subcutaneously allografted tumors circled for clarity. Large pores are visible in a subset of the treatment groups. At the same time point, FFPE tumor sections were prepared and subjected to immunohistochemical staining for granzyme B and perforin (scale bar: 1 mm). (D) Image intensity quantitation for granzyme B (left) and perforin (right), $n = 3\text{--}4$ per cohort. The mean relative intensity value for each cohort is displayed above the plots. Error bars represent the SEM; * $p < 0.05$ and ** $p < 0.01$ by one-way ANOVA.

degranulation causes release of perforin, which promotes pore formation on the tumor cell membrane, allowing granzyme B to access the cytosol and proteolytically activate proapoptotic Bcl-2 family members.^{29–32} Tumors from mice treated with the specific RNAi and antibody combination were highly positive for both biomarkers (Figure 2C), compared to tumors from the placebo or monotherapy cohorts. Interestingly, large pores were observed on the tumors macroscopically in the B16F10 cohorts treated with the antibodies, consistent with the effects of polymerized perforin as has been reported for metastatic melanoma patients on cell-based immunotherapy (Figure 2C; T. Schumacher, 2018, *Mol. Cancer Ther.*, abstract).³³

To further investigate the mechanism by which this experimental drug combination yields antitumor efficacy, the B16F10 tumor study shown in Figure 2A was repeated two additional times under independent conditions where the syngeneic tumor did not have access to host T cells (Figure S2). In the first case, CD8-positive T cells were depleted by treatment with a CD8a-targeting monoclonal antibody (mAb) before and during combination therapy, as previously described³⁵ (Figure S2A). In parallel, the experimental regimen was repeated in tumor-bearing athymic nu/nu (nude) mice, which natu-

rally lack T lymphocytes (Figure S2B). In both of these studies, no tumor growth inhibition was observed with the combination or with either single agent. These data demonstrate that RNAi-mediated sensitization to immune checkpoint inhibition is completely dependent on the presence of cytotoxic T cells.

RNAi Potentiation of Checkpoint Blockade Is Independent of Dysregulated Wnt Signaling and Does Not Require anti-CTLA-4

Aberrant Wnt signaling, often detected by the steady-state presence of β -catenin in the tumor cell nucleus, results in a dissociation between extracellular stimuli and Wnt-dependent mitogenic transcriptional programming. In tumors without dysregulated Wnt signaling, β -catenin is only detected in the membrane or in a diffuse cytosolic pattern. Human cancers featuring aberrant Wnt signaling due to a tumorigenic genetic lesion, a category that includes >95% of colorectal tumors and smaller percentages of other tumor types, are sometimes referred to as Wnt activated.²⁷ In human tumor xenograft models, silencing of *CTNNB1* mRNA by therapeutic RNAi only yields antitumor efficacy in the Wnt-activated context.¹⁹

Given these past observations, we sought to determine if activated Wnt is a prerequisite for DCR-BCAT plus immunotherapy combination

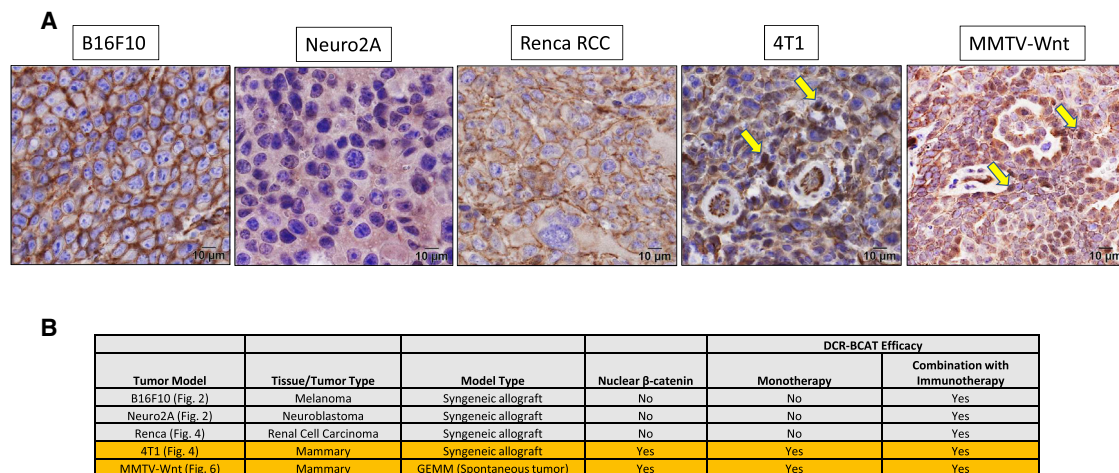


Figure 3. Correlation between Nuclear β -Catenin and DCR-BCAT Activity in Murine Tumors

(A) Representative high-magnification images of FFPE tumor sections stained for murine β -catenin. All five tumor models used in this paper are included. Yellow arrows show examples of nuclear stain, which is only clearly visible in a subset of tumor cells in the 4T1 and MMTV-Wnt models. In the absence of nuclear β -catenin, the blue hematoxylin from the H&E counterstain is visible in the nucleus. Scale bars: 10 μ m. (B) The 5 models used in this paper, showing that presence of nuclear β -catenin is required for DCR-BCAT-mediated antitumor efficacy as a monotherapy, but its ability to potentiate the response to checkpoint blockade was independent of this parameter. The antitumor efficacy data are from Figures 2, 4, 6, and 7 of the current paper.

efficacy. First, we determined which of the models used in our experiments were positive for nuclear β -catenin (Figure 3). Interestingly and unexpectedly, B16F10 and Neuro2A tumors are highly responsive to combination therapy (Figure 2), despite their lack of detectable nuclear β -catenin (Figure 3). We then sought to clarify this correlation using additional models. We selected two additional models for subcutaneous allografting: 4T1 breast tumors, which are Wnt activated due to their loss of the negative regulator Wnt5A,³⁶ and Renca renal cell carcinoma (RCC), which have no reported evidence of Wnt activation and an absence of nuclear β -catenin (Figure 3). Interestingly, flow cytometry data from Wnt-activated 4T1 tumors (Figure S3) showed a similar level of checkpoint elevation after RNAi treatment as B16F10 (Figure S1). Consistent with their likely Wnt activation status, 4T1, but not Renca, tumors displayed sensitivity to DCR-BCAT monotherapy (Figures 4A and 4B). Critically, both models were relatively insensitive to immunotherapy alone, but they demonstrated highly significant TGI (74%) in the RNAi combination setting (Figures 4A and 4B). These data again suggest a broad applicability for DCR-BCAT in combination with immunotherapy and that genetic background is not a dominant driver of response.

Given the observation that steady-state nuclear β -catenin was not required for its immune modulating function in tumors, we explored a possible role for indirect, noncanonical mechanisms. β -catenin is known to interact directly with nuclear factor κ B (NF- κ B) transcription complexes and inhibit its transcriptional activity through sequestration, an event that may contribute to immunosuppression in a subset of liver, breast, and colorectal tumors.^{37–39} Chemokines CXCL10 and CXCL11 are known to be highly responsive to NF- κ B signaling.⁴⁰ Intriguingly, we observed that systemic DCR-BCAT therapy caused upregulation of the corresponding mRNAs encoding

these chemokines, *Cxcl10* and *Cxcl11*, in multiple models in a Wnt-independent manner (Figure S4). These observations offer the suggestion that one or more known noncanonical β -catenin-signaling mechanisms are involved in its tumor T cell exclusion activity.^{37–39}

As part of the same line of experimentation, we also sought to further characterize RNAi combination therapy by determining if comparable efficacy is achieved by inhibiting PD-1 alone compared to PD-1 + CTLA-4. PD-1 alone is a favorable treatment option due to its higher therapeutic index compared to anti-CTLA-4 therapy.^{41,42} Importantly, in both 4T1 and Renca, the potentiation of response by RNAi was similar if the immunotherapy regimen used both antibodies or was limited to anti-PD-1 alone (Figures 4A and 4B). Taken together, DCR-BCAT demonstrates considerable versatility in sensitizing diverse tumors to multiple immunotherapy regimens.

Characterization of DCR-BCAT-Mediated Immunomodulation in Spontaneous MMTV-Wnt1 Tumors

DCR-BCAT is an LNP drug product. Biodistribution, including tumor extravasation and penetration, is highly dependent on the physical properties of nanoparticles.⁴³ A well-known liability of surgical tumor models (xenografts and allografts) is the uncertainty that the tumor has developed a clinically representative microenvironment and vasculature.⁴⁴ Therefore, it is critical that our findings are validated in a spontaneous tumor setting, where the TME is not influenced by the allografting process. For this series of studies, we employed the MMTV-Wnt1 mammary model, as these tumors are highly β -catenin dependent.^{45,46} MMTV-Wnt1 mice develop palpable mammary tumors within several months of birth, and with near complete penetrance. MMTV-Wnt1 tumors are also expected to be immunologically cold due to their low mutational load.⁴⁷

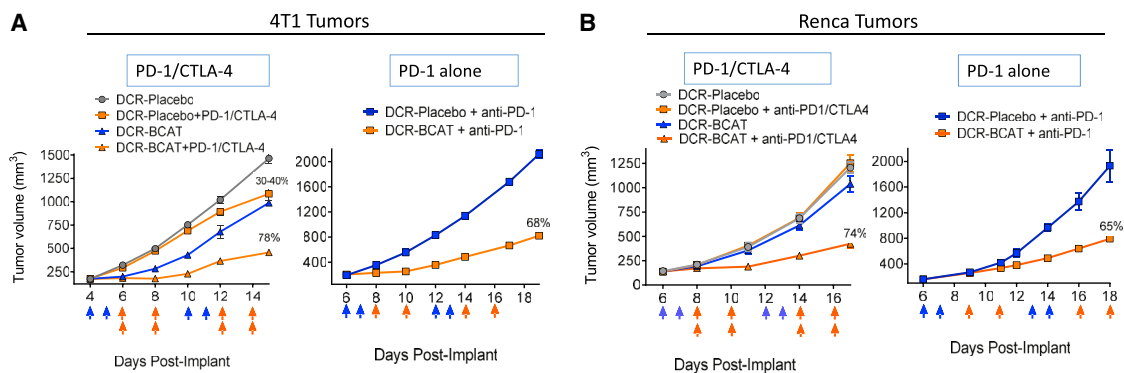


Figure 4. Anti-PD-1 Therapy Alone Is Sufficient to Sensitize Tumors to DCR-BCAT

4T1 (A) or Renca (B) tumor-bearing mice ($n = 5$ /cohort) were generated and enrolled as described. Dosing was initiated when tumor volume reached 100–300 mm³. Animals were dosed on the days indicated by the arrows (blue arrows, DCR-BCAT or DCR-Placebo, 3 mg/kg/dose; orange arrows, anti-PD-1/CTLA-4, 5 mg/kg/dose of each antibody in the combination cohorts only as indicated in the figure). For the PD-1 alone studies (right panels of A and B), anti-PD-1 was administered at a 5 mg/kg/dose. DCR-BCAT and DCR-Placebo were given intravenously (tail vein) and the antibodies were administered intraperitoneally. Tumor volumes were measured twice weekly over the study period. The mean TGI values are displayed on the plots for the cohorts that responded to therapy. Error bars represent the SEM and are sometimes too small to be visible on the plots.

First, MMTV-Wnt1 mice with well-established tumors were treated with DCR-BCAT (5 mg/kg, qdx3), and tumor sections were stained for both β -catenin and CD8 (Figure 5A). At the protein level, near-complete loss of β -catenin was observed throughout the tumor section. In the absence of RNAi treatment, cytotoxic T cells (CD8) were virtually undetectable, whereas after treatment, the tumors were highly CD8 positive, similar to our observations from allografted tumors (Figure 1). To characterize the kinetics and dose dependence of T cell recruitment following *Cttnb1* silencing, we used qPCR to track *Cttnb1* and *Cd8a* mRNA levels after treating animals with different dose regimens and dose levels (Figure 5B). These data showed that a single dose of 3 mg/kg was insufficient to affect levels of either mRNA. Two daily doses of either 3 or 5 mg/kg was sufficient to detect a decrease in *Cttnb1* and a simultaneous increase in *Cd8a*. Adding a second cycle of two daily doses further increased the magnitude of the *Cd8a* response. Finally, similar mRNA responses were observed if the measurements were taken either 1 or 4 days after the final dose, demonstrating a durable pharmacodynamic signal. In addition to *Cd8a*, other markers of tumor inflammation, including *Cd274* (PD-L1) mRNA, as well as known IFN γ -responsive mRNAs *Cxcl10*, *Stat1*, and *Ido1* mRNAs,⁴⁸ were also elevated by DCR-BCAT under these conditions (Figure S5). These findings support the adaptive immune resistance hypothesis in which the PD-L1 is not constitutively expressed but induced in response to inflammatory signals such as IFN γ that are produced by an active antitumor immune response mediated by CD8+ T cells.^{49,50}

Antitumor Efficacy of DCR-BCAT Monotherapy and Combination Immunotherapy in MMTV-Wnt1 Mice

To determine the effect of DCR-BCAT as a single agent on the growth of MMTV-Wnt1 tumors, we treated mice with palpable mammary tumors (200–400 mm³) with 3 daily doses of 3 mg/kg (Figure 6, left panel). While the DCR-Placebo cohort displayed approximately

5-fold increases in tumor volume in less than a week after the final dose, complete TGI was observed in the DCR-BCAT cohort. At day 9 of the study, a crossover protocol was employed where the animals with large tumors from the DCR-Placebo cohort (1,500–2,500 mm³) were treated with DCR-BCAT (Figure 6, right panel). Again, complete stasis in tumor growth was observed, suggesting that tumor size does not affect the pharmacological activity of this drug product.

In a follow-up study, DCR-BCAT or DCR-Placebo was tested in combination with PD-1/CTLA-4 immunotherapy (Figure 7A, left panel). In this experiment, the number of RNAi doses per cycle was decreased from 3 to 2, to tune the monotherapy antitumor response from complete TGI to partial TGI, thus enabling a larger dynamic range to observe the effects of combination therapy. Immunotherapy alone yielded a minimal response, consistent with the lack of detectable CD8+ T cells in MMTV-Wnt1 tumors. To the contrary, DCR-BCAT combined with immunotherapy yielded complete TGI and near-complete tumor regression in 3 of 5 tumors in the cohort (Figure 7A, left panel). Administration of maintenance therapy in the 3 complete responders (two additional cycles) resulted in a lack of palpable tumors in these animals up to 1 month after study initiation (Figure 7A, right panel). A tumor excised from animals on therapy was positive for CD8, perforin, and granzyme B 1 day after the completion of the second cycle (Figure 7B), suggesting a T cell cytotoxicity mechanism similar to observations in B16F10 allografted tumors (Figure 2). Collectively, these data serve to demonstrate that *Cttnb1* silencing is a robust strategy to sensitize CD8-negative tumors to immunotherapy in clinically relevant models.

Indirect Wnt Pathway Targeting Is Not Sufficient for Inhibiting Immune Exclusion in Non-Wnt-Activated Tumors

While DCR-BCAT targets β -catenin directly via post-transcriptional mRNA silencing, several clinical-stage Wnt pathway modulators are

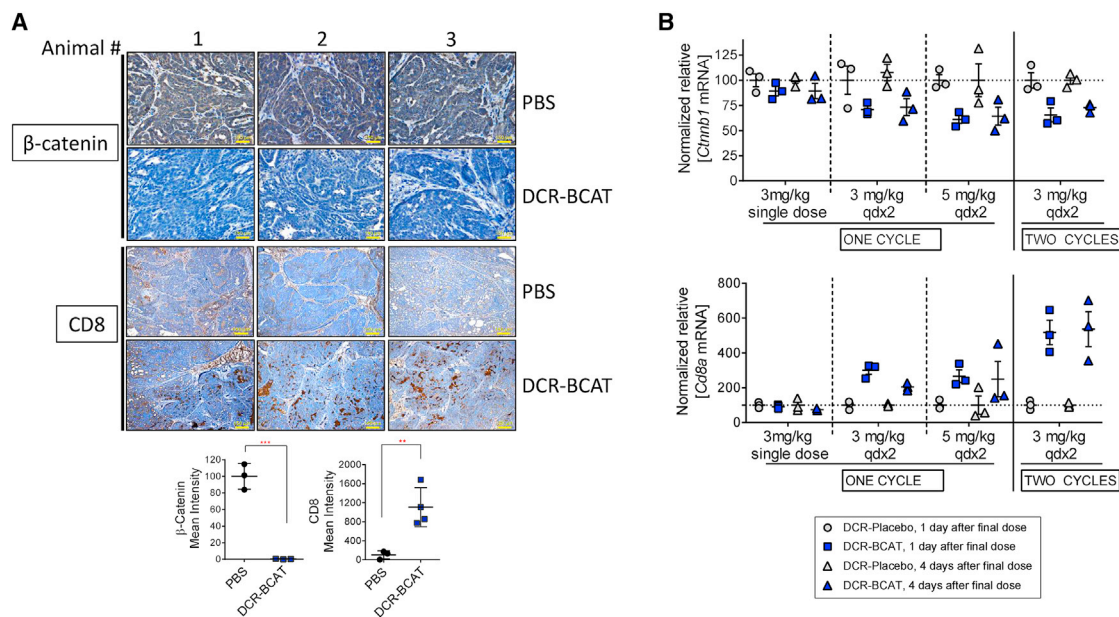


Figure 5. DCR-BCAT Increases Tumor CD8+ T Cells in Spontaneous MMTV-Wnt1 Tumors

(A) FFPE sections were prepared from mammary tumors excised from MMTV-Wnt1 mice dosed intravenously with DCR-BCAT (5 mg/kg qdx3, $n = 3$), followed by immunohistochemical staining for β -catenin (top) and CD8 (bottom) and image acquisition. Mean intensity values are plotted and displayed. Scale bars: 150 μ m. (B) Tumor-bearing MMTV-Wnt1 mice were dosed intravenously with DCR-BCAT or DCR-Placebo for various regimens and cycle numbers ($n = 3$ per condition), as shown. Tumors were harvested for RNA isolation either one (gray symbols) or four (blue symbols) days after the final dose was administered. qPCR was performed to measure normalized relative expression of *Ctnnb1* (top) and *Cd8a* (bottom) mRNAs.

being evaluated for their ability to promote antitumor efficacy through indirect β -catenin inhibition.^{27,51–53} One such investigational drug (and arguably the most clinically advanced), LGK-974, is an inhibitor of the PORCN acetyltransferase, which is required for secretion of Wnt ligands.⁵⁴ LGK-974 has been in multiple clinical trials, including in combination with anti-PD-(L)1, for evaluation as a potentiator of immune checkpoint inhibition. We sought to compare the ability of LGK-974 and DCR-BCAT to promote T cell infiltration. To perform this comparison, we employed mice harboring two relevant tumor types: Wnt-active tumors driven by overexpression of a Wnt ligand and, therefore, predicted to be responsive to LGK-974 (MMTV-Wnt1 model) and non-Wnt-activated tumors (B16F10) (Figure 8; Figure S6). This analysis utilized *Axin2* mRNA as a surrogate for Wnt activity, due to its excellent correlation with Wnt signatures and nuclear β -catenin in humans,¹⁴ and *Cd8a* mRNA to monitor tumor T cell content.

In MMTV-Wnt1 tumors, the Wnt effector mRNA *Axin2* was suppressed by both DCR-BCAT and LGK-974 at dose levels previously reported⁵⁴ to be efficacious (Figures 8A and 8B). The pharmacodynamic response to LGK-974, however, is very transient as previously shown,⁵⁴ presumably due to its pharmacokinetic properties; *Axin2* mRNA returns to baseline by 24 hr after treatment (Figure 8B). Predictably, only DCR-BCAT directly affected *Ctnnb1* mRNA levels as LGK-974 does not target *Ctnnb1* mRNA or β -catenin protein directly. Importantly, *Cd8a* mRNA elevation was observed after

both direct and indirect inhibition. T cell elevation appeared to be variable but sustained 24 hr after LGK-974 treatment, suggesting that even a transient dampening of Wnt activity is sufficient for this mechanism (Figure 8B). However, the T cell response was far more robust and consistent between animals after repeat dosing of LGK-974, compared to a single administration (Figure 8B). These data suggest that suppression of β -catenin by direct or indirect pharmacological intervention is sufficient to overcome its immune evasion function in tumors that are driven by Wnt ligand defects, although such genetic lesions are relatively uncommon in humans.²⁷

It is worth noting that one limitation of LGK-974 is that, as an inhibitor of Wnt ligand secretion, it is expected to be generally ineffective against the majority of Wnt-activated tumors. This is because most tumors in this category are driven by downstream genetic lesions such as *APC*, which is by far the most common mutation found in colorectal tumors. Indeed, while DCR-BCAT reduces expression of both *CTNNB1* (63%) and *AXIN2* (58%) in LS411N colorectal cancer (CRC) human tumor xenografts (3 doses of 1 mg/kg) harboring an *APC* loss-of-function mutation¹⁹ (Figure 8C), LGK-974 caused only a slight, transient reduction of *AXIN2* (19%) in LS411N tumors even at highly exaggerated dose levels (9 daily doses of 3 mg/kg). These data further exemplify the broad potential of the direct-targeting RNAi approach.

In non-Wnt-driven B16F10 tumors, DCR-BCAT treatment demonstrated a similar reduction of *Ctnnb1* mRNA but no effect on *Axin2*

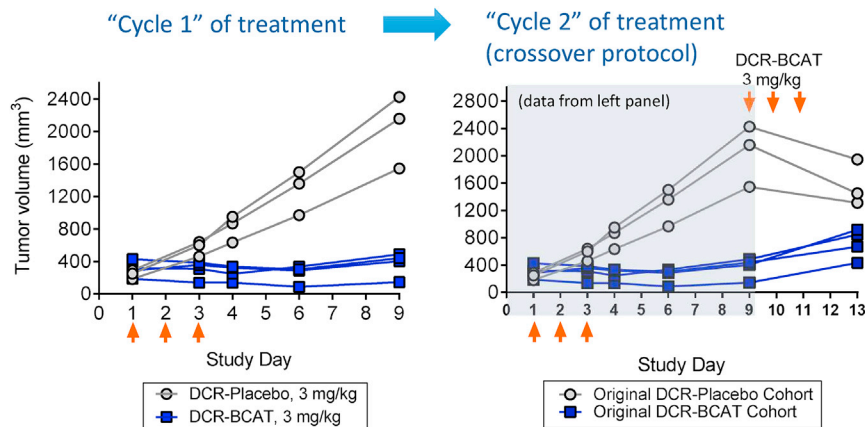


Figure 6. Efficacy of DCR-BCAT in Small and Large MMTV-Wnt1 Tumors as a Monotherapy

MMTV-Wnt1 tumor-bearing mice were randomized and enrolled in an antitumor efficacy study. Animals were dosed intravenously with DCR-BCAT ($n = 4$) or DCR-Placebo ($n = 3$) at 3 mg/kg qdx3. Caliper measurements were taken periodically and the data for each individual animal are plotted (left panel). 6 days after the final dose was administered, a crossover protocol was initiated (right panel), where the DCR-Placebo animals were treated with DCR-BCAT and vice versa (3 mg/kg, qdx3).

mRNA (Figure S6), as predicted given the lack of steady-state nuclear β -catenin (Figure 3). Despite the lack of direct transcriptional effects, direct inhibition of β -catenin yielded tumor T cell infiltration (Figure 1; Figure S6). To the contrary, LGK-974 was unable to promote an increase in *Cd8a* mRNA, suggesting that pathway perturbation at the level of Wnt ligand secretion does not promote immune modulation in contexts where β -catenin function is not dysregulated (Figure S6). These stark differences suggest that the broad applicability of DCR-BCAT in potentiating immunotherapy across tumors of diverse genetic origin does not extend to indirect Wnt pathway modulators.

DISCUSSION

Increasing the response rate to immune checkpoint inhibition is arguably the most important long-term goal in experimental medical oncology. Numerous lines of evidence suggest that direct targeting of tumor-intrinsic pathways, including Wnt/ β -catenin and other classical oncogenes, could be a highly impactful strategy to achieve favorable outcomes to immunotherapy. First, multiple independent investigators have reported an inverse correlation between Wnt signaling and tumor T cell infiltration across a spectrum of human tumors.^{13,14,51,55–57} Functionally, the modulation of β -catenin expression has been shown to have a large impact on tumor T cell content in preclinical models.¹³ Similarly, oncogenic RAS signaling drives immunosuppression by increasing the stability of *PD-L1* mRNA.⁵⁸ Indeed, in clinical studies of RAS/RAF-activated tumors, treatments with downstream BRAF and MEK inhibitors have also increased T cell infiltration.^{58–60} MYC depletion also appears to confer immunologic benefit,^{17,61} as well as histone deacetylase (HDAC) inhibitors, which may modulate oncogene expression through epigenetic mechanisms.⁶² Finally, loss-of-function mutations in tumor suppressors, including PTEN, p53, and LKB1, also appear to correlate negatively with tumor T cell content.⁶³ Collectively, these observations validate the emerging strategy of rational drug combinations to sensitize tumors to anti-PD-1, anti-PD-L1, and other emerging checkpoint inhibitors.

Despite this emerging evidence, direct and tumor-selective intervention to potentiate immunotherapy has been extremely challenging.

Clinical evaluation of the BRAF inhibitor vemurafenib in combination with the CTLA-4 antibody ipilimumab was terminated early because of substantial liver toxicities.⁶⁴ While MEK inhibition (MEKi) may be better tolerated,⁶⁵ there is the concern that MEKi can paradoxically suppress T cell activation through nonspecific systemic effects.^{66,67} Efforts to target MYC and β -catenin^{51,54,68,69} are thus far indirect, non-tumor selective, and in some cases appear to have toxicity liabilities due to unwanted pharmacology in normal tissues.⁵⁴ DCR-BCAT and its underlying LNP technology offer two significant potential advantages over these approaches. Namely, pharmacological activity is limited in most normal tissues, and equally important is that the technology enables direct targeting of a classically un-drug-treatable oncogene. Both of these attributes may increase the therapeutic index while limiting signaling redundancy and acquired resistance. While the RNAi approach for this application overcomes some limitations of conventional drug modalities, challenges remain, including limited clinical experience, the relative complexity of PK/PD relationships, and the higher cost of manufacturing. Along with DCR-BCAT, ongoing preclinical programs investigating KRAS-targeting oligonucleotides^{70,71} will also contribute to the collective experience in this rapidly emerging space.

The work in this report corroborates the central components of the mechanism proposed by Spranger et al.,¹³ but our observations uncovered a key difference with clinical implications. The previous work strongly suggests that dysregulated Wnt/ β -catenin signaling is required for immunomodulation. Intriguingly, our work demonstrates that RNAi therapy sensitizes tumors to checkpoint inhibition even in the absence of activated Wnt signaling, greatly increasing the number of potentially eligible patients. While more work is needed to understand the factors that contribute to this apparent discrepancy, these observations suggest a role for one or more of the numerous functions of β -catenin beyond its canonical transcriptional activity at TCF/LEF promoter sites. Clearly, important mechanistic questions remain. We have corroborated that β -catenin causes suppression of CCL4 and other chemokines, which in turn limits the ability of tumors from recruiting APCs or T cells directly.^{13,63} APCs, including dendritic cells, function not only by presenting the antigens to T cells but also by promoting recruitment of T cells to the TME.⁶³ An important line of investigation will be to determine if β -catenin

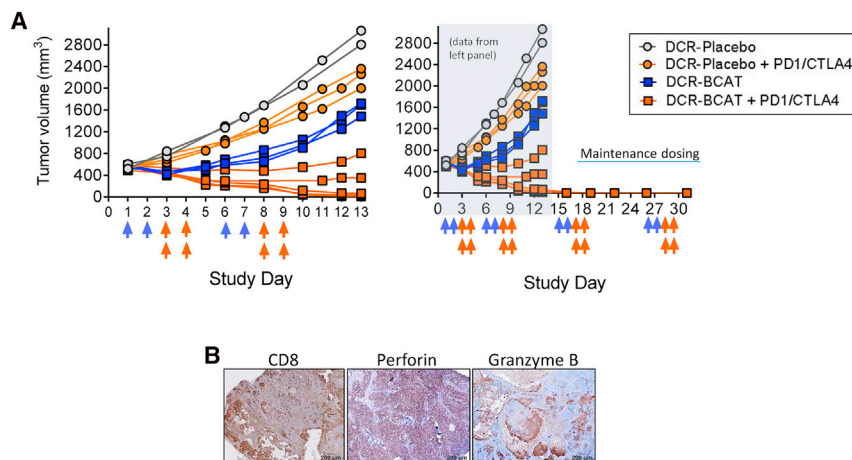


Figure 7. Efficacy of DCR-BCAT in MMTV-Wnt1 Tumors in Combination with Immunotherapy

(A) MMTV-Wnt1 tumor-bearing mice were randomized into four cohorts ($n = 2-5$, as shown) and enrolled in an antitumor efficacy study. The tumor volume at study initiation ranged from 400 to 600 mm³. Animals were dosed on the days indicated by the arrows (blue arrows, DCR-BCAT or DCR-Placebo, 3 mg/kg/dose; orange arrows, anti-PD-1/CTLA-4, 5 mg/kg/dose of each antibody in the combination cohorts only as indicated in the figure, left panel). DCR-BCAT and DCR-Placebo were given intravenously (tail vein) and the antibodies were administered intraperitoneally. Tumor volumes were measured frequently during the study period, and the measurements for the individual animals are shown. For the 3 of 5 animals in the combination cohort (orange squares) that achieved complete regression, animals were placed on maintenance therapy for an additional

two cycles (right panel). (B) A satellite animal from the DCR-BCAT + PD-1/CTLA-4 combination cohort was necropsied on day 10, 24 hr after the final antibody dose. FFPE slides were prepared and stained for CD8, perforin, and granzyme B as indicated. Scale bars: 200 μ m.

also promotes immune evasion through non-CCL4-dependent mechanisms. One reasonably well-characterized indirect pathway that could be contributing to the phenotype is the sequestration of NF- κ B by β -catenin,³⁷ resulting in the suppression of T cell-attracting chemokines, including CXCL10 and others.^{40,72} It is likely that the pharmacological inhibition of β -catenin in the non-Wnt-activated setting reverses its suppression of inflammatory genes, in part, by restoring the NF- κ B.³⁷ Interestingly, NF- κ B is also known to cross-talk with the ATF3 transcriptional repressor, possibly explaining the effects on CCL4 even in the non-Wnt-activated context.⁷³

In addition to their ability to promote T cell exclusion by restricting antigen presentation, tumors are known to promote an immunosuppressive microenvironment containing T_{regs}, MDSCs, and subtypes of tumor-associated macrophages (TAMs), all of which can directly or indirectly inactivate CD8⁺ T cells.^{74,75} While preliminary evidence would not suggest a major role for MDSCs (Figures S1 and S2), this is still an open area of experimentation. If β -catenin is found to affect recruitment of immunosuppressive cells to the TME, adding other classes of immunotherapeutics to the RNAi-containing regimen, including IDO1 inhibitors or STING agonists, may further improve responses.⁷⁶⁻⁷⁸ RNAi and the advanced LNP drug delivery technology will also continue to serve as powerful research tools for elucidating these outstanding questions in preclinical tumor models.

Previous work demonstrated that the modular nature of the LNP encapsulated RNAi platform enables rational targeting of specific oncogenes or combinations thereof, potentially based on personalized genetic profiling of individual tumors. In this report, we demonstrate that the combination of systemically administered therapeutic RNAi and common immunotherapeutics may yield striking efficacy in difficult-to-treat, immunotherapy-refractory tumors independently of genetic background. Overall, this study provides a strong rationale for clinical evaluation of this novel treatment strategy.

MATERIALS AND METHODS

Materials

All DsiRNAs were synthesized by Integrated DNA Technologies (IDT, Coralville, IA). Primer and probe oligonucleotides used in real-time qPCR detection were synthesized by IDT or Life Technologies (Carlsbad, CA). Monoclonal antibodies (anti-mouse PD-1, anti-mouse CTLA-4, and anti-mouse CD8 α) were purchased from Bio X Cell (Lebanon, NH). Tumor dissociation kit and Smart Strainers used to make single-cell suspension were purchased from Miltenyi Biotec (Bergisch Gladbach, Germany). Monoclonal antibodies used for flow cytometry were purchased from BioLegend (San Diego, CA). DCR-BCAT and Placebo LNPs were prepared as previously described.¹⁹ Anti PD-1 antibody, anti-CTLA-4 antibodies, and anti-CD8a antibodies were diluted in PBS and administered intraperitoneally. DCR-BCAT and DCR-Placebo (LNP with chemistry-matched, scrambled *CTNNT1* DsiRNA) were given intravenously. LGK-974 was purchased from Selleckchem.com (Houston, TX). LGK-974 was dissolved in DMSO (2%) and Corn Oil (solvents added individually and in order) and was administered orally.

Cell Lines

Mouse cell lines B16F10, 4T1, Neuro 2A (N2A), and Renca were obtained from ATCC (Manassas, VA). B16F10 and cells were grown in DMEM supplemented with 10% fetal bovine serum (FBS). 4T1 and Renca cell lines were grown in RPMI medium supplemented with 10% FBS. N2A cells were grown in MEM supplemented with 10% FBS. C57BL/6 and BALB/c mice were obtained from Charles River Laboratories (Indianapolis, IN) and A/J mice were obtained from The Jackson Laboratory (Bar Harbor, ME). All cell lines were maintained at 37°C and 5% CO₂. All cells were tested regularly for mycoplasma contamination and for rodent pathogens.

Murine Tumor Models

For syngeneic allograft models, 6- to 8-week-old C57BL/6, BALB/c, and A/J mice were injected subcutaneously with B16F10 (1×10^6 cells),

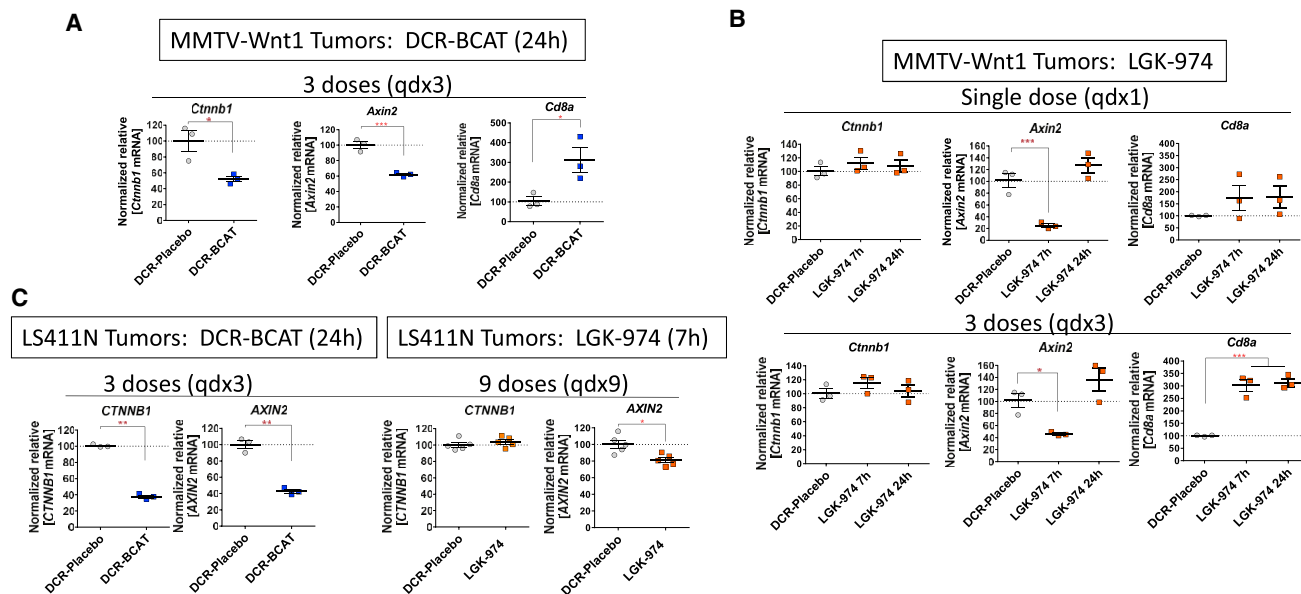


Figure 8. Both DCR-BCAT and Indirect Wnt Pathway Inhibition Enable Tumor T Cell Recruitment in MMTV-Wnt1 Tumors

MMTV-Wnt1 tumor-bearing mice were intravenously treated with DCR-BCAT (A) or orally with LGK974 (B) at 3 mg/kg/dose using the indicated dose regimens. 24 hr (A and bottom panel of B) or 7 hr (top panel of B) after the last dose, tumors were collected and total RNA was extracted and subjected to qPCR analysis for relative expression of specific mRNAs as indicated. (C) Immunocompromised nu/nu (nude) mice harboring LS411N colorectal xenograft tumors were treated with DCR-BCAT (1 mg/kg qdx3, one cycle), as described previously,¹⁹ or LGK-974 (3 mg/kg, qdx9) and collected 7 hr post-final dose. Total RNA was extracted and subjected to qPCR analysis for relative expression of *CTNNB1* and *AXIN2* mRNAs. Error bars represent the SEM; **p* < 0.05, ***p* < 0.01, ****p* < 0.001 by unpaired t test and one-way ANOVA; *n* = 3–5 per cohort.

Renca (1×10^6 cells), 4T1 (2×10^6 cells), or N2A (2×10^6 cells) under the right shoulder. For Figure S2B only, athymic nu/nu mice were used as indicated. The appropriate background strain was chosen for each syngeneic tumor type, based on ATCC guidance. Dosing was initiated when the tumors reached 100–300 mm³. Tumor volume was measured 2–3 times a week. For transgenic model experiments, MMTV-Wnt1 mice harboring a *Wnt1* transgene under control of the mouse mammary tumor virus long terminal repeat (MMTV-LTR) promoter in a C57BL/6 background (B6SJL-Tg (Wnt1)1Hev/J)⁷⁹ were obtained from The Jackson Laboratory. The mice were palpated twice a week to detect mammary tumor formation. When the tumors reached a volume of 200–500 mm³, mice were divided randomly into cohorts and treated with PBS, DCR-Placebo, or DCR-BCAT, according to the dosing regimens described in the Results. The LNP encapsulated DsiRNAs were dosed intravenously via lateral tail vein at a total volume of 10 mL/kg. Anti PD-1 and anti-CTLA-4 antibodies were given intraperitoneally at 10 mL/kg. For the CD8 α depletion study, B16F10 tumor-bearing C57BL/6 mice were injected intraperitoneally with CD8 α monoclonal antibody at 200 μ g/mouse on days 4 and 5 post-tumor implantation, followed by 4 maintenance doses at 100 μ g/mouse every fourth day throughout the experiment. The studies were performed in the LS411N xenograft model as described previously.¹⁹ Mice were held in a pathogen-free environment, and all procedures involving animals were performed according to protocols approved by Dicerna Pharmaceuticals' Institutional Animal Care and Use Committee (Dicerna-IACUC).

qRT-PCR Measurements

Animal tissues were preserved by either snap-freezing or by fixing in RNA-later solution (Life Technologies, Carlsbad, CA), and they were homogenized using a QIAGEN TissueLyzer bead mill (Germantown, MD). After total RNA isolation, representative RNA samples were subjected to quality control (QC) and determination of the RNA Integrity Number (RIN) score by Agilent 2100 Bioanalyzer. 100 ng total RNA was used to make cDNA using high-capacity cDNA Reverse Transcription Kit (Applied Biosystems, Carlsbad, CA). The cDNA was then diluted 4 times for qRT-PCR using TaqMan Fast Advanced Master Mix (Applied Biosystems) and murine gene-specific primer-probe sets. The following primer-probe sets from Life Technologies were used: *Ctnnb1* (Mm00483039_m1), mouse *Cd8a* (Mm01182107_g1), mouse *Ccl4* (Mm00443111_m1), mouse *Pdcd1* (Mm01285676_m1), mouse *Cd274* (Mm00452054_m1), mouse *Cd247* (Mm00446171_m1), mouse *Ppib* (Mm00478295_m1), mouse *Cxcl10* (Mm00445235_m1), mouse *Cxcl11* (Mm00444662_m1), *Cxcl9* (Mm00434946_m1), *Stat1* (Mm01257286_m1), *Ido1* (Mm00492590_m1), *Ifng* (Mm01168134_m1), human *CTNNB1* (Hs00355045_m1), and human *AXIN2* (Hs00610344_m1). In some experiments, Superscript III one-step qRT-PCR kit (Applied Biosystems, 11732-088) was used as well.

IHC

FFPE tissue sections were stained with primary antibodies and Signal Stain DAB substrate kit (Cell Signaling Technology, 8059)

to do IHC analysis as described previously.¹⁹ For staining, antibodies against β -catenin (Cell Signaling Technology, Danvers, MA; 8480), CD8 (Invitrogen, Rockford, IL; MA5-13473), granzyme B (Santa Cruz Biotechnology, Dallas, TX; sc-8022), perforin (Santa Cruz Biotechnology, Dallas, TX; sc-7417), as well as the chromatin stain DAPI were used at a concentration of 1:500. Image quantification was performed using Nikon NIS-Elements Advanced Research (AR) software; each data point is the mean of three independent sum intensity measurements taken from representative fields.

Flow Cytometry

Tumors were isolated from mice 24 hr after the final dose of the described regimen. Freshly collected tumors were then disaggregated using GentleMACS mouse tumor dissociation kit (Miltenyi Biotec, Auburn, CA) and filtered through a 70- μ m nylon cell strainer to generate single-cell suspension. All tumor cells were then stained with a viability dye and with fluorescent dye-conjugated antibodies in PBS for 20 min on ice. Antibodies to CD3 (17A2), CD4 (GK1.5), CD8 α (53-6.7), PD-1 (29F.1A12), CD103 (2E7), CD11b (M1/70), CD25 (PC81), Tim-3 (B8.2C12), LAG-3 (C9B7W), CD16/32 (93), and NK-1.1 (PK136) were purchased from BioLegend (San Diego, CA). Data were acquired on an LSR II flow cytometer (Becton Dickinson, Franklin Lakes, NJ) and analyzed using FlowJo software (Ashland, OR).

Statistical Analysis

All the data are reported as the sample mean \pm SEM. Comparisons between two groups were performed using unpaired t test (two tailed, unpaired). Multiple comparisons were performed using one-way ANOVA in GraphPad Prism software.

SUPPLEMENTAL INFORMATION

Supplemental Information includes six figures and can be found with this article online at <https://doi.org/10.1016/j.ymthe.2018.09.005>.

AUTHOR CONTRIBUTIONS

S.G., W.W., B.D.B., and M.T.A. conceived and designed experiments. S.G. and X.S. performed the experiments. S.G., X.S., K.P.C., J.P., W.W., and M.T.A. analyzed the data. S.G., X.S., and W.W. contributed reagents, material, and analysis tools. S.G., B.D.B., and M.T.A. wrote and revised the manuscript.

CONFLICTS OF INTEREST

All authors are full-time employees and shareholders of Dicerna Pharmaceuticals.

ACKNOWLEDGMENTS

The authors would like to thank Douglas Fambrough, Pankaj Bhargava, Bart Wise, Jim Weissman, Naim Nazef, Hank Dudek, Cheng Lai, Girish Chopda, Chaitali Dutta, and Martin Koser for support, guidance, and feedback and Geremew Desta for help with animal husbandry. This study was funded in part by National Cancer Institute (NCI) SBIR grant IR43CA186410-02.

REFERENCES

- Chen, D.S., and Mellman, I. (2013). Oncology meets immunology: the cancer-immunity cycle. *Immunity* 39, 1–10.
- Chen, L., and Han, X. (2015). Anti-PD-1/PD-L1 therapy of human cancer: past, present, and future. *J. Clin. Invest.* 125, 3384–3391.
- Sharma, P., and Allison, J.P. (2015). The future of immune checkpoint therapy. *Science* 348, 56–61.
- Lu, J., Lee-Gabel, L., Nadeau, M.C., Ferencz, T.M., and Soefje, S.A. (2015). Clinical evaluation of compounds targeting PD-1/PD-L1 pathway for cancer immunotherapy. *J. Oncol. Pharm. Pract.* 21, 451–467.
- Hegde, P.S., Karanikas, V., and Evers, S. (2016). The Where, the When, and the How of Immune Monitoring for Cancer Immunotherapies in the Era of Checkpoint Inhibition. *Clin. Cancer Res.* 22, 1865–1874.
- Gajewski, T.F. (2015). The Next Hurdle in Cancer Immunotherapy: Overcoming the Non-T-Cell-Inflamed Tumor Microenvironment. *Semin. Oncol.* 42, 663–671.
- Hassel, J.C., Heinzelinger, L., Aberle, J., Bähr, O., Eigentler, T.K., Grimm, M.O., Grünwald, V., Leipe, J., Reinmuth, N., Tietze, J.K., et al. (2017). Combined immune checkpoint blockade (anti-PD-1/anti-CTLA-4): Evaluation and management of adverse drug reactions. *Cancer Treat. Rev.* 57, 36–49.
- Gadgeel, S.M., Shields, A.F., Heilbrun, L.K., Labadidi, S., Zalupski, M., Chaplen, R., and Philip, P.A. (2003). Phase II study of paclitaxel and carboplatin in patients with advanced gastric cancer. *Am. J. Clin. Oncol.* 26, 37–41.
- Koo, T., and Kim, I.A. (2016). Radiotherapy and immune checkpoint blockades: a snapshot in 2016. *Radiat. Oncol. J.* 34, 250–259.
- Mazzone, R., Zwergel, C., Mai, A., and Valente, S. (2017). Epi-drugs in combination with immunotherapy: a new avenue to improve anticancer efficacy. *Clin. Epigenetics* 9, 59.
- Deken, M.A., Gadiot, J., Jordanova, E.S., Lacroix, R., van Gool, M., Kroon, P., Pineda, C., Geukes Foppen, M.H., Scolyer, R., Song, J.Y., et al. (2016). Targeting the MAPK and PI3K pathways in combination with PD1 blockade in melanoma. *OncolImmunology* 5, e1238557.
- Lyou, Y., Habowski, A.N., Chen, G.T., and Waterman, M.L. (2017). Inhibition of nuclear Wnt signalling: challenges of an elusive target for cancer therapy. *Br. J. Pharmacol.* 174, 4589–4599.
- Spranger, S., Bao, R., and Gajewski, T.F. (2015). Melanoma-intrinsic β -catenin signaling prevents anti-tumour immunity. *Nature* 523, 231–235.
- Grasso, C.S., Giannakis, M., Wells, D.K., Hamada, T., Mu, X.J., Quist, M., Nowak, J.A., Nishihara, R., Qian, Z.R., Inamura, K., et al. (2018). Genetic mechanisms of immune evasion in colorectal cancer. *Cancer Discov.* 8, 730–749.
- Sumimoto, H., Takano, A., Teramoto, K., and Daigo, Y. (2016). RAS-Mitogen-Activated Protein Kinase Signal Is Required for Enhanced PD-L1 Expression in Human Lung Cancers. *PLoS ONE* 11, e0166626.
- Peng, W., Chen, J.Q., Liu, C., Malu, S., Creasy, C., Tetzlaff, M.T., Xu, C., McKenzie, J.A., Zhang, C., Liang, X., et al. (2016). Loss of PTEN Promotes Resistance to T Cell-Mediated Immunotherapy. *Cancer Discov.* 6, 202–216.
- Casey, S.C., Tong, L., Li, Y., Do, R., Walz, S., Fitzgerald, K.N., Gouw, A.M., Baylot, V., Güttgemann, I., Eilers, M., and Felsner, D.W. (2016). MYC regulates the antitumor immune response through CD47 and PD-L1. *Science* 352, 227–231.
- Bobbin, M.L., and Rossi, J.J. (2016). RNA Interference (RNAi)-Based Therapeutics: Delivering on the Promise? *Annu. Rev. Pharmacol. Toxicol.* 56, 103–122.
- Ganesh, S., Koser, M.L., Cyr, W.A., Chopda, G.R., Tao, J., Shui, X., Ying, B., Chen, D., Pandya, P., Chipumuro, E., et al. (2016). Direct Pharmacological Inhibition of β -Catenin by RNA Interference in Tumors of Diverse Origin. *Mol. Cancer Ther.* 15, 2143–2154.
- Ganesh, S., Shui, X., Craig, K.P., Koser, M.L., Chopda, G.R., Cyr, W.A., Lai, C., Dudek, H., Wang, W., Brown, B.D., and Abrams, M.T. (2018). β -catenin mRNA silencing and MEK inhibition display synergistic efficacy in preclinical tumor models. *Mol. Cancer Ther.* 17, 544–553.
- Chen, S., Lee, L.F., Fisher, T.S., Jessen, B., Elliott, M., Evering, W., Logronio, K., Tu, G.H., Tzavarikos, K., Li, X., et al. (2015). Combination of 4-1BB agonist

- and PD-1 antagonist promotes antitumor effector/memory CD8 T cells in a poorly immunogenic tumor model. *Cancer Immunol. Res.* 3, 149–160.
22. Guillerey, C., Huntington, N.D., and Smyth, M.J. (2016). Targeting natural killer cells in cancer immunotherapy. *Nat. Immunol.* 17, 1025–1036.
 23. Topalian, S.L., Drake, C.G., and Pardoll, D.M. (2015). Immune checkpoint blockade: a common denominator approach to cancer therapy. *Cancer Cell* 27, 450–461.
 24. Huang, A.C., Postow, M.A., Orlowski, R.J., Mick, R., Bengsch, B., Manne, S., Xu, W., Harmon, S., Giles, J.R., Wenz, B., et al. (2017). T-cell invigoration to tumour burden ratio associated with anti-PD-1 response. *Nature* 545, 60–65.
 25. Curran, M.A., Montalvo, W., Yagita, H., and Allison, J.P. (2010). PD-1 and CTLA-4 combination blockade expands infiltrating T cells and reduces regulatory T and myeloid cells within B16 melanoma tumors. *Proc. Natl. Acad. Sci. USA* 107, 4275–4280.
 26. Damsky, W.E., Curley, D.P., Santhanakrishnan, M., Rosenbaum, L.E., Platt, J.T., Gould Rothberg, B.E., Taketo, M.M., Dankort, D., Rimm, D.L., McMahon, M., and Bosenberg, M. (2011). β -catenin signaling controls metastasis in Braf-activated Pten-deficient melanomas. *Cancer Cell* 20, 741–754.
 27. Zhan, T., Rindtorff, N., and Boutros, M. (2017). Wnt signaling in cancer. *Oncogene* 36, 1461–1473.
 28. Rigo, V., Emionite, L., Daga, A., Astigiano, S., Corrias, M.V., Quintarelli, C., Locatelli, F., Ferrini, S., and Croce, M. (2017). Combined immunotherapy with anti-PDL-1/PD-1 and anti-CD4 antibodies cures syngeneic disseminated neuroblastoma. *Sci. Rep.* 7, 14049.
 29. Hiebert, P.R., and Granville, D.J. (2012). Granzyme B in injury, inflammation, and repair. *Trends Mol. Med.* 18, 732–741.
 30. Martínez-Lostao, L., Anel, A., and Pardo, J. (2015). How Do Cytotoxic Lymphocytes Kill Cancer Cells? *Clin. Cancer Res.* 21, 5047–5056.
 31. Gordy, C., and He, Y.W. (2012). Endocytosis by target cells: an essential means for perforin- and granzyme-mediated killing. *Cell. Mol. Immunol.* 9, 5–6.
 32. Rousalova, I., and Krepela, E. (2010). Granzyme B-induced apoptosis in cancer cells and its regulation (review). *Int. J. Oncol.* 37, 1361–1378.
 33. Kelderman, S., Heemskerck, B., Fanchi, L., Philips, D., Toebe, M., Kvistborg, P., van Buuren, M.M., van Rooij, N., Michels, S., Germeroth, L., et al. (2016). Antigen-specific TIL therapy for melanoma: A flexible platform for personalized cancer immunotherapy. *Eur. J. Immunol.* 46, 1351–1360.
 35. Holmgaard, R.B., Schaer, D.A., Li, Y., Castaneda, S.P., Murphy, M.Y., Xu, X., Inigo, I., Dobkin, J., Manro, J.R., Iversen, P.W., et al. (2018). Targeting the TGF β pathway with galunisertib, a TGF β RI small molecule inhibitor, promotes anti-tumor immunity leading to durable, complete responses, as monotherapy and in combination with checkpoint blockade. *J. Immunother. Cancer* 6, 47.
 36. Jiang, W., Crossman, D.K., Mitchell, E.H., Sohn, P., Crowley, M.R., and Serra, R. (2013). WNT5A inhibits metastasis and alters splicing of Cd44 in breast cancer cells. *PLoS ONE* 8, e58329.
 37. Deng, J., Miller, S.A., Wang, H.Y., Xia, W., Wen, Y., Zhou, B.P., Li, Y., Lin, S.Y., and Hung, M.C. (2002). β -catenin interacts with and inhibits NF- κ B in human colon and breast cancer. *Cancer Cell* 2, 323–334.
 38. Du, Q., Zhang, X., Cardinal, J., Cao, Z., Guo, Z., Shao, L., and Geller, D.A. (2009). Wnt/ β -catenin signaling regulates cytokine-induced human inducible nitric oxide synthase expression by inhibiting nuclear factor- κ B activation in cancer cells. *Cancer Res.* 69, 3764–3771.
 39. Moreau, M., Mourah, S., and Dosquet, C. (2011). β -Catenin and NF- κ B cooperate to regulate the uPA/uPAR system in cancer cells. *Int. J. Cancer* 128, 1280–1292.
 40. Huang, H., Langenkamp, E., Georganaki, M., Loskog, A., Fuchs, P.F., Dieterich, L.C., Kreuger, J., and Dimberg, A. (2015). VEGF suppresses T-lymphocyte infiltration in the tumor microenvironment through inhibition of NF- κ B-induced endothelial activation. *FASEB J.* 29, 227–238.
 41. Swart, M., Verbrugge, I., and Beltman, J.B. (2016). Combination Approaches with Immune-Checkpoint Blockade in Cancer Therapy. *Front. Oncol.* 6, 233.
 42. El Osta, B., Hu, F., Sadek, R., Chintalapally, R., and Tang, S.C. (2017). Not all immune-checkpoint inhibitors are created equal: Meta-analysis and systematic review of immune-related adverse events in cancer trials. *Crit. Rev. Oncol. Hematol.* 119, 1–12.
 43. Bhise, K., Sau, S., Alsaab, H., Kashaw, S.K., Tekade, R.K., and Iyer, A.K. (2017). Nanomedicine for cancer diagnosis and therapy: advancement, success and structure-activity relationship. *Ther. Deliv.* 8, 1003–1018.
 44. Wartha, K., Herting, F., and Hasmann, M. (2014). Fit-for purpose use of mouse models to improve predictivity of cancer therapeutics evaluation. *Pharmacol. Ther.* 142, 351–361.
 45. Proffitt, K.D., Madan, B., Ke, Z., Pendharkar, V., Ding, L., Lee, M.A., Hannoush, R.N., and Virshup, D.M. (2013). Pharmacological inhibition of the Wnt acyltransferase PORCN prevents growth of WNT-driven mammary cancer. *Cancer Res.* 73, 502–507.
 46. Yu, Q.C., Verheyen, E.M., and Zeng, Y.A. (2016). Mammary Development and Breast Cancer: A Wnt Perspective. *Cancers (Basel)* 8, E65.
 47. Champiat, S., Ferté, C., Lebel-Binay, S., Eggermont, A., and Soria, J.C. (2014). Exomics and immunogenics: Bridging mutational load and immune checkpoints efficacy. *Oncol Immunology* 3, e27817.
 48. Ayers, M., Lunceford, J., Nebozhyn, M., Murphy, E., Loboda, A., Kaufman, D.R., Albright, A., Cheng, J.D., Kang, S.P., Shankaran, V., et al. (2017). IFN- γ -related mRNA profile predicts clinical response to PD-1 blockade. *J. Clin. Invest.* 127, 2930–2940.
 49. Pardoll, D.M. (2012). The blockade of immune checkpoints in cancer immunotherapy. *Nat. Rev. Cancer* 12, 252–264.
 50. Topalian, S.L., Taube, J.M., Anders, R.A., and Pardoll, D.M. (2016). Mechanism-driven biomarkers to guide immune checkpoint blockade in cancer therapy. *Nat. Rev. Cancer* 16, 275–287.
 51. Schatoff, E.M., Leach, B.I., and Dow, L.E. (2017). Wnt Signaling and Colorectal Cancer. *Curr. Colorectal Cancer Rep.* 13, 101–110.
 52. Novellasademunt, L., Antas, P., and Li, V.S. (2015). Targeting Wnt signaling in colorectal cancer. A Review in the Theme: Cell Signaling: Proteins, Pathways and Mechanisms. *Am. J. Physiol. Cell Physiol.* 309, C511–C521.
 53. Zhang, X., and Hao, J. (2015). Development of anticancer agents targeting the Wnt/ β -catenin signaling. *Am. J. Cancer Res.* 5, 2344–2360.
 54. Liu, J., Pan, S., Hsieh, M.H., Ng, N., Sun, F., Wang, T., Kasibhatla, S., Schuller, A.G., Li, A.G., Cheng, D., et al. (2013). Targeting Wnt-driven cancer through the inhibition of Porcupine by LGK974. *Proc. Natl. Acad. Sci. USA* 110, 20224–20229.
 55. Luke, J.J., Bao, R., Spranger, S., Sweis, R.F., and Gajewski, T. (2016). Correlation of WNT/ β -catenin pathway activation with immune exclusion across most human cancers. *J. Clin. Oncol.* 34, 3004.
 56. Sharma, P., Hu-Lieskovan, S., Wargo, J.A., and Ribas, A. (2017). Primary, Adaptive, and Acquired Resistance to Cancer Immunotherapy. *Cell* 168, 707–723.
 57. Pai, S.G., Carneiro, B.A., Mota, J.M., Costa, R., Leite, C.A., Barroso-Sousa, R., Kaplan, J.B., Chae, Y.K., and Giles, F.J. (2017). Wnt/ β -catenin pathway: modulating anti-cancer immune response. *J. Hematol. Oncol.* 10, 101.
 58. Coelho, M.A., de Carné Trécesson, S., Rana, S., Zecchin, D., Moore, C., Molina-Arcas, M., East, P., Spencer-Dene, B., Nye, E., Barnouin, K., et al. (2017). Oncogenic RAS Signaling Promotes Tumor Immuno-resistance by Stabilizing PD-L1 mRNA. *Immunity* 47, 1083–1099.e6.
 59. Koya, R.C., Mok, S., Otte, N., Blacketer, K.J., Comin-Anduix, B., Tume, P.C., Minasyan, A., Graham, N.A., Graeber, T.G., Chodon, T., and Ribas, A. (2012). BRAF inhibitor vemurafenib improves the antitumor activity of adoptive cell immunotherapy. *Cancer Res.* 72, 3928–3937.
 60. Cooper, Z.A., Juneja, V.R., Sage, P.T., Frederick, D.T., Piris, A., Mitra, D., Lo, J.A., Hodi, F.S., Freeman, G.J., Bosenberg, M.W., et al. (2014). Response to BRAF inhibition in melanoma is enhanced when combined with immune checkpoint blockade. *Cancer Immunol. Res.* 2, 643–654.
 61. Topper, M.J., Vaz, M., Chiappinelli, K.B., DeStefano Shields, C.E., Niknafs, N., Yen, R.C., Wenzel, A., Hicks, J., Ballew, M., Stone, M., et al. (2017). Epigenetic Therapy Ties MYC Depletion to Reversing Immune Evasion and Treating Lung Cancer. *Cell* 171, 1284–1300.e21.
 62. Terranova-Barberio, M., Thomas, S., Ali, N., Pawlowska, N., Park, J., Krings, G., Rosenblum, M.D., Budillon, A., and Munster, P.N. (2017). HDAC inhibition potentiates immunotherapy in triple negative breast cancer. *Oncotarget* 8, 114156–114172.

63. Spranger, S., and Gajewski, T.F. (2018). Impact of oncogenic pathways on evasion of antitumor immune responses. *Nat. Rev. Cancer* *18*, 139–147.
64. Ribas, A., Hodi, F.S., Callahan, M., Konto, C., and Wolchok, J. (2013). Hepatotoxicity with combination of vemurafenib and ipilimumab. *N. Engl. J. Med.* *368*, 1365–1366.
65. Su, F., Viros, A., Milagre, C., Trunzer, K., Bollag, G., Spleiss, O., Reis-Filho, J.S., Kong, X., Koya, R.C., Flaherty, K.T., et al. (2012). RAS mutations in cutaneous squamous-cell carcinomas in patients treated with BRAF inhibitors. *N. Engl. J. Med.* *366*, 207–215.
66. Boni, A., Cogdill, A.P., Dang, P., Udayakumar, D., Njauw, C.N., Sloss, C.M., Ferrone, C.R., Flaherty, K.T., Lawrence, D.P., Fisher, D.E., et al. (2010). Selective BRAFV600E inhibition enhances T-cell recognition of melanoma without affecting lymphocyte function. *Cancer Res.* *70*, 5213–5219.
67. Vella, L.J., Pasam, A., Dimopoulos, N., Andrews, M., Knights, A., Puaux, A.L., Louahed, J., Chen, W., Woods, K., and Cebon, J.S. (2014). MEK inhibition, alone or in combination with BRAF inhibition, affects multiple functions of isolated normal human lymphocytes and dendritic cells. *Cancer Immunol. Res.* *2*, 351–360.
68. Delmore, J.E., Issa, G.C., Lemieux, M.E., Rahl, P.B., Shi, J., Jacobs, H.M., Kastriitis, E., Gilpatrick, T., Paranal, R.M., Qi, J., et al. (2011). BET bromodomain inhibition as a therapeutic strategy to target c-Myc. *Cell* *146*, 904–917.
69. Emami, K.H., Nguyen, C., Ma, H., Kim, D.H., Jeong, K.W., Eguchi, M., Moon, R.T., Teo, J.L., Kim, H.Y., Moon, S.H., et al. (2004). A small molecule inhibitor of beta-catenin/CREB-binding protein transcription [corrected]. *Proc. Natl. Acad. Sci. USA* *101*, 12682–12687.
70. Kamekar, S., LeBleu, V.S., Sugimoto, H., Yang, S., Ruivo, C.F., Melo, S.A., Lee, J.J., and Kalluri, R. (2017). Exosomes facilitate therapeutic targeting of oncogenic KRAS in pancreatic cancer. *Nature* *546*, 498–503.
71. Ross, S.J., Revenko, A.S., Hanson, L.L., Ellston, R., Staniszewska, A., Whalley, N., Pandey, S.K., Reville, M., Rooney, C., Buckett, L.K., et al. (2017). Targeting KRAS-dependent tumors with AZD4785, a high-affinity therapeutic antisense oligonucleotide inhibitor of KRAS. *Sci. Transl. Med.* *9*, eaal5253.
72. Muthuswamy, R., Berk, E., Junecko, B.F., Zeh, H.J., Zureikat, A.H., Normolle, D., Luong, T.M., Reinhart, T.A., Bartlett, D.L., and Kalinski, P. (2012). NF- κ B hyperactivation in tumor tissues allows tumor-selective reprogramming of the chemokine microenvironment to enhance the recruitment of cytolytic T effector cells. *Cancer Res.* *72*, 3735–3743.
73. Hoessel, B., and Schmid, J.A. (2013). The complexity of NF- κ B signaling in inflammation and cancer. *Mol. Cancer* *12*, 86.
74. Whiteside, T.L., Demaria, S., Rodriguez-Ruiz, M.E., Zarour, H.M., and Melero, I. (2016). Emerging Opportunities and Challenges in Cancer Immunotherapy. *Clin. Cancer Res.* *22*, 1845–1855.
75. Munn, D.H., and Bronte, V. (2016). Immune suppressive mechanisms in the tumor microenvironment. *Curr. Opin. Immunol.* *39*, 1–6.
76. Smyth, M.J., Ngiow, S.F., Ribas, A., and Teng, M.W. (2016). Combination cancer immunotherapies tailored to the tumour microenvironment. *Nat. Rev. Clin. Oncol.* *13*, 143–158.
77. Hennequart, M., Pilotte, L., Cane, S., Hoffmann, D., Stroobant, V., Plaen, E., and Van den Eynde, B.J. (2017). Constitutive IDO1 Expression in Human Tumors Is Driven by Cyclooxygenase-2 and Mediates Intrinsic Immune Resistance. *Cancer Immunol. Res.* *5*, 695–709.
78. Corrales, L., Matson, V., Flood, B., Spranger, S., and Gajewski, T.F. (2017). Innate immune signaling and regulation in cancer immunotherapy. *Cell Res.* *27*, 96–108.
79. Tsukamoto, A.S., Grosschedl, R., Guzman, R.C., Parslow, T., and Varmus, H.E. (1988). Expression of the int-1 gene in transgenic mice is associated with mammary gland hyperplasia and adenocarcinomas in male and female mice. *Cell* *55*, 619–625.